

Massive Meson Fluctuation in NJL Model

Mei Huang¹, Pengfei Zhuang², Weiqin Chao^{1,3}

¹ Institute of High Energy Physics, Chinese Sciences Academy, Beijing 100039, China

² Physics Department, Tsinghua University, Beijing 100084, China

³ CCAST, Beijing 100080, China

(October 8, 2018)

Based on the self-consistent scheme beyond mean-field approximation in the large N_c expansion, including current quark mass explicitly, a general scheme of SU(2) NJL model is developed. To ensure the quark self-energy expanded in the proper order of N_c , an approximate internal meson propagator is deduced, which is in order of $O(1/N_c)$. In our scheme, adopting the method of external momentum expansion, all the Feynman diagrams are calculated in a unified way by only expanding the quark propagator. Our numerical results show, that different from the mean field approximation in which the explicitly chiral symmetry breaking is invisible, the effect of finite pion mass can be seen clearly when beyond mean-field approximation.

I. INTRODUCTION

As we all know, chiral symmetry breaking was originally explained quite well by Nambu-Jona-Lasinio (NJL) model as early as 1961 [1]. Like in superconductivity, the strong attractive force between quark and antiquark in the $J^P = 0^+$ channel can create non-perturbative ground state with $\bar{q}q$ condensation. Due to the pair condensation, the original symmetry between massless left and right-handed quarks is broken down to $U_V(N_f)$, and then the quarks obtain constituent mass. The remaining residual interactions between the constituent quarks bind them into collective excitations, i.e., hadrons in the chiral symmetry breaking vacuum. Especially in the pseudoscalar channel the residual strong interaction creates massless pions as Goldstone bosons in the chiral limit. When a small current quark mass m_0 is introduced in the theory, chiral symmetry is explicitly broken, and pion obtains its small physical mass m_π .

Although the NJL model has two serious drawbacks, i.e., lacks of confinement and renormalizability, it is still regarded as an applicable model at low momentum, especially for dealing with processes of pion, such as pion-pion scattering near threshold.

Traditionally, the scheme of the NJL model is represented by two Schwinger-Dyson (SD) equations, one is for the constituent quark propagator, and the other is for the composite meson propagator. At the lowest level, the applications of the NJL model are based upon mean-field approximation [2] - [7], i.e., Hartree approximation to the gap equation for quark mass and the random-phase approximation (RPA) to the Bethe-Salpeter equation for meson mass. It is clear, that at this level the solution of the gap equation determines the meson propagators, but the solution of meson SD equation has no feedback to the quark propagator. Since the constituent quark propagator is the fundamental element, from which all the quantities, including quark mass, meson masses and quark-antiquark condensate, are calculated, it is necessary to consider the back contribution of meson modes to the quark propagator.

Among efforts [8] - [14] to go beyond the mean-field approximation, Refs. [12] and [13]

are in a chirally symmetric self-consistent approximation, namely the chiral properties such as the Goldstone's theorem, the Goldberger-Treiman relation and the conservation of the quark axial current are exactly preserved in the chiral limit of the NJL model. By using effective action method in a semi-bosonized way, and expanding the action to one quark-loop and one-meson-loop in [12], or directly evaluating the Feynman diagrams under the constraint to keep the chiral relations at quark level in [13].

In this paper, we extend the method of [13] to a general scheme with explicit chiral symmetry breaking in the SU(2) NJL model. Different from the case in the chiral limit, we must be careful to deal with the form of internal meson propagators. In a way different from [13], we regard the constituent quark as the fundamental element and only expand quark's propagator in the power of small external momentum in the calculation of Feynman diagrams.

In the process to go beyond the mean-field approximation, we have to deal with the divergent integrals of quark loops and meson loops. We adopt Pauli-Villars regulation [3,15] to treat divergent integrals resulted from quark loops, and choose a covariant cutoff Λ_b for the meson momentum. There are four parameters in our treatment, namely the current quark mass m_0 , quark coupling constant G , fermionic cut-off Λ_f and bosonic cut-off Λ_b , to be fixed. In the mean-field approximation, the three parameters m_0 , G , Λ_f are usually fixed by comparing with the pion mass $m_\pi = 140$ MeV, pion decay constant $f_\pi = 92.4$ MeV and the quark condensate $1/2 < \bar{q}q >^{1/3} = -250$ MeV. In the near future, the DIRAC experiment will measure the $\pi - \pi$ scattering lengths in good precision, which will shed some light on the quark condensate [16]. To see clearly the quark condensate dependence of the four parameters, we give only the quark condensate a reasonable constraint: $-300 \text{ MeV} \sim -200 \text{ MeV}$.

The outline of this paper is as follows: In section 2, we briefly review the general scheme represented by two Schwinger-Dyson equations in the SU(2) NJL model. In Section 3, we introduce the method of external momentum expansion, and prove a general relation between the pion polarization function and the axial-vector matrix element. We also deduce

the internal meson propagator to $O(1/N_c)$ order in the N_c expansion. Our numerical results with mesonic contributions and the effect of explicit chiral symmetry breaking will be shown in section 4. The conclusions are given at the end.

II. THE FUNDAMENTAL SCHEME IN SU(2) NJL MODEL

A. Two Schwinger-Dyson equations in SU(2) NJL model

In this section, we briefly review the traditional scheme of SU(2) NJL model with large N_c expansion. The two-flavor NJL model is defined through the Lagrangian density,

$$\mathcal{L} = \bar{\psi}(i\gamma^\mu\partial_\mu - m_0)\psi + G[(\bar{\psi}\psi)^2 + (\bar{\psi}i\gamma_5\vec{\tau}\psi)^2], \quad (1)$$

here G is the effective coupling constant of dimension GeV^{-2} , and m_0 is the current quark mass, assuming isospin degeneracy of the u and d quarks, and $\psi, \bar{\psi}$ are quark fields with flavor, colour and spinor indices suppressed.

The traditional non-perturbative method of NJL model is inspired from many-body theory. The complete description is represented by two Schwinger-Dyson (SD) integral equations, i.e., the constituent quark propagator, see Fig. 1a, and the composite meson propagator, see Fig. 1b.

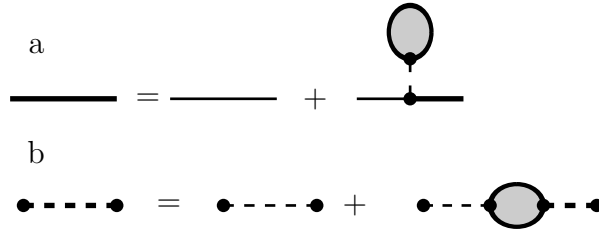


FIG. 1. The two Schwinger-Dyson equations for the quark propagator a and the meson propagator b . The light dashed lines in a and b represent the four-fermion vertex $2iG$, and the one-vertex gray bubble in a and the two-vertex gray bubble in b indicate the quark self-energy and the meson polarization function respectively.

The two SD equations must couple to each other self-consistently and keep chiral symmetry in the chiral limit. The one-vertex grey bubble *kernel a* in Fig. 1a represents the quark self-energy, and the two-vertex grey bubble *kernel b* in Fig. 1b indicates the meson polarization function. In the case of SU(2), meson modes refer to only pseudoscalar mesons π and scalar mesons σ .

It is difficult to give the full expressions of *kernel a* and *kernel b* in Fig. 1. Usually an approximation scheme called large N_c expansion is adopted in NJL model, i.e., the both kernels expanded in $1/N_c$, where N_c is the number of color. In this scheme, GN_c is a constant when $N_c \rightarrow \infty$, so coupling constant scales like $G \sim N_c^{-1}$. One can find the detailed description of large N_c expansion in [17,9]. V.Dmitrašinović et.al. proved in their paper [13] that the *kernel a* and *kernel b* shown in Fig. 2 are self-consistent leading and subleading order in N_c expansion and can keep all the chiral relations in the chiral limit.

The leading $O(1)$ order of quark self-energy *kernel a* in Fig. 2 is named m_H after Hartree approximation, and the subleading $O(1/N_c)$ order is called δm . Including current quark mass m_0 , the gap equation for quarks can be expressed as

$$m = m_0 + m_H + \delta m, \quad (2)$$

where $m_H = 16imGN_cF$, and F is given in Appendix in order to compactly discuss physics in the text.

The leading $O(N_c)$ and subleading $O(1)$ order of meson polarization function *kernel b* are expressed as $\Pi_M^{(RPA)}(k)$ and $\delta\Pi_M(k)$ respectively, here M represents π or σ . It is clear to see that the back interaction which conserves all the chiral properties is reflected in the contribution from the meson propagator to the quark mass. The total meson propagator can be expressed in terms of the total polarization function

$$-iD_M(k) = \frac{2iG}{1 - 2G\Pi_M(k)}, \quad (3)$$

where $\Pi_M(k) = \Pi_M^{(RPA)}(k) + \delta\Pi_M(k)$, and the RPA part is $\Pi_\pi^{(RPA)}(k) = 8iN_cF - 4iN_ck^2I(k)$ for π and $\Pi_\sigma^{(RPA)}(k) = 8iN_cF - 4iN_c(k^2 - 4m^2)I(k)$ for σ , and the function $I(k)$ is defined in Appendix.

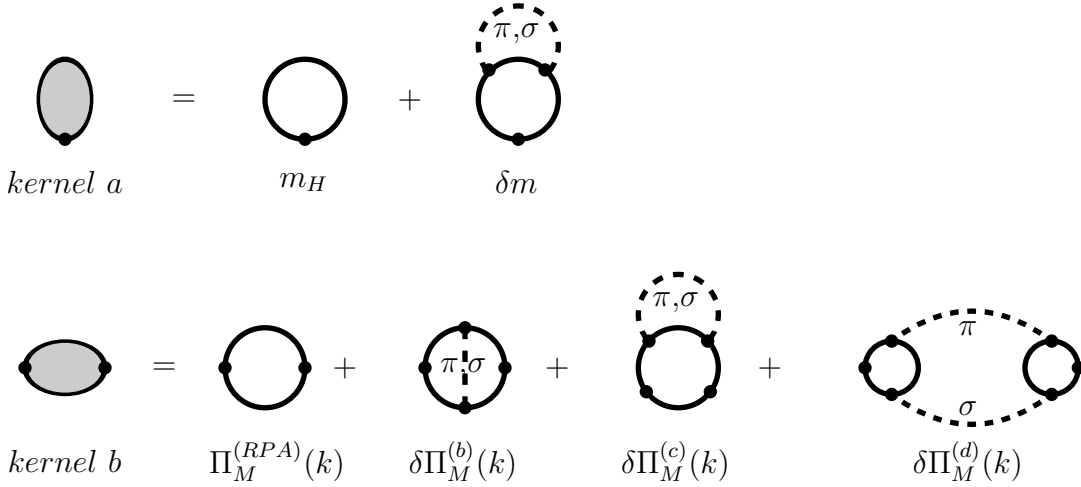


FIG. 2. *kernel a* and *kernel b* in the quark and meson propagators. m_H and δm are the leading and subleading contributions to the quark mass. $\Pi_M^{(RPA)}$ and $\delta\Pi_M^{(b,c,d)}$ are the leading and subleading order contributions to meson polarization function. The heavy solid lines indicate the constituent quark propagator, and the heavy dashed lines represent π or σ propagator $-iD_M^{(RPA)}(q)$ in RPA approximation.

In the NJL model, mesons are bound states of constituent quark and anti-quark, the meson mass m_M satisfies the meson propagator's pole condition

$$1 - 2G\Pi_M(k^2 = m_M^2) = 0, \quad (4)$$

and the coupling constant g_{Mqq} is determined by the residue at the pole

$$g_{Mqq}^{-2} = (\partial\Pi_M(k)/\partial k^2)^{-1}|_{k^2=m_M^2}. \quad (5)$$

Performing direct calculation of the Feynman diagrams in Fig. 2 leads to the explicit expressions for the quark mass

$$\begin{aligned} -i\delta m &= 12GN_c \int \frac{d^4q}{(2\pi)^4} [-iD_\pi^{(RPA)}(q)] \int \frac{d^4p}{(2\pi)^4} \text{Tr}[\gamma_5 S(p+q)\gamma_5 S(p)1S(p)] \\ &\quad - 4GN_c \int \frac{d^4q}{(2\pi)^4} [-iD_\sigma^{(RPA)}(q)] \int \frac{d^4p}{(2\pi)^4} \text{Tr}[1S(p+q)1S(p)1S(p)], \end{aligned} \quad (6)$$

and for pion polarization fluctuations

$$\begin{aligned}\delta\Pi_\pi^{(b)}(k) = & 2iN_c \left[\int \frac{d^4q}{(2\pi)^4} [-iD_\pi^{(RPA)}(q)] \int \frac{d^4p}{(2\pi)^4} \text{Tr}[\gamma_5 S(p+q)\gamma_5 S(p)\gamma_5 S(p-k)\gamma_5 S(p-k+q)] \right. \\ & \left. + \int \frac{d^4q}{(2\pi)^4} [-iD_\sigma^{(RPA)}(q)] \int \frac{d^4p}{(2\pi)^4} \text{Tr}[\gamma_5 S(p+q)1S(p)\gamma_5 S(p-k)1S(p-k+q)] \right], \quad (7)\end{aligned}$$

$$\begin{aligned}\delta\Pi_\pi^{(c)}(k) = & -12iN_c \left[\int \frac{d^4q}{(2\pi)^4} [-iD_\pi^{(RPA)}(q)] \int \frac{d^4p}{(2\pi)^4} \text{Tr}[\gamma_5 S(p)\gamma_5 S(p+q)\gamma_5 S(p)\gamma_5 S(p-k)] \right. \\ & \left. - \frac{1}{3} \int \frac{d^4q}{(2\pi)^4} [-iD_\sigma^{(RPA)}(q)] \int \frac{d^4p}{(2\pi)^4} \text{Tr}[\gamma_5 S(p)1S(p+q)1S(p)\gamma_5 S(p-k)] \right], \quad (8)\end{aligned}$$

$$\delta\Pi_\pi^{(d)}(k) = i \int \frac{d^4q}{(2\pi)^4} [-i\Gamma^{\sigma\pi\pi}(k, q)] [-iD_\pi^{(RPA)}(q)] [-iD_\sigma^{(RPA)}(q-k)] [-i\Gamma^{\sigma\pi\pi}(q, k)]. \quad (9)$$

Here, the expression $\Gamma^{\sigma\pi\pi}(k, q)$ is the $(\sigma\pi\pi)$ -vertex

$$-i\Gamma^{\sigma\pi\pi}(k, q) = -4N_c i \int \frac{d^4p}{(2\pi)^4} \text{Tr}[\gamma_5 S(p+k)1S(p+q)\gamma_5 S(p)], \quad (10)$$

$S(p) = 1/(\not{p} - m)$ the quark propagator and $-iD_{\pi,\sigma}^{(RPA)}(q)$ the internal meson propagator. In all the formulae of this paper, k means the π external momentum, p the internal quark momentum and q the internal meson momentum;

B. Pion Decay Constant

Another important quantity is the pion decay constant f_π which is calculated from the vacuum to one-pion axial-vector matrix element, replacing one vertex $i\gamma_5\vec{\tau}$ of *kernel* b in Fig. 2 by $ig_{\pi qq}(k)\gamma_5\gamma_\mu\vec{\tau}/2$. Similar to the expression of $\Pi_\pi(k)$, we express $f_\pi(k)$ as

$$\begin{aligned}f_\pi(k) &= f_\pi^{(RPA)}(k) + \delta f_\pi(k) \\ &= f_\pi^{(RPA)}(k) + \delta f_\pi^{(b)}(k) + \delta f_\pi^{(c)}(k) + \delta f_\pi^{(d)}(k).\end{aligned} \quad (11)$$

Since the Feynman diagrams for $\Pi_\pi(k)$ and f_π have the same structure, we expect to find a general relation between them. Starting from the axial-vector matrix element $\langle 0|J_{\mu 5}^i|\pi^j(k)\rangle = if_\pi(k)k_\mu\delta^{ij}$, and using the single-quark axial Ward identity involving the quark propagator $S(p)$,

$$\gamma_5 \not{k} = 2m\gamma_5 + \gamma_5 S^{-1}(p+k) + S^{-1}(p)\gamma_5, \quad (12)$$

one can deduce the general relations functions

$$\begin{aligned}\frac{k^2 f_\pi^{(RPA)}(k)}{g_{\pi qq}(k)} &= m\Pi_\pi^{(RPA)}(k) - \frac{m_H}{2G}, \\ \frac{k^2 \delta f_\pi(k)}{g_{\pi qq}(k)} &= m\delta\Pi_\pi(k) - \frac{\delta m}{2G}.\end{aligned}\tag{13}$$

The detailed proof can be found in Ref. [13]. Using pion's pole condition Eq. (4) and gap equation Eq. (2), we get finally the relation

$$\frac{m_\pi^2 f_\pi}{g_{\pi qq}} = \frac{m_0}{2G},\tag{14}$$

where we have defined the on-shell quantities $f_\pi = f_\pi(k^2 = m_\pi^2)$, $g_{\pi qq} = g_{\pi qq}(k^2 = m_\pi^2)$.

While in the chiral limit, f_π satisfies the Goldberger-Treiman relation $f_\pi g_{\pi qq} = m$.

III. EXTERNAL MOMENTUM EXPANSION

A. Method of External Momentum Expansion

We are familiar with one-loop Feynman diagrams, but it is difficult to analytically calculate the two-loop Feynman diagrams such as those in *kernel b*. Since pion's external momentum $k^2 = m_\pi^2$ is small, we will calculate the subleading corrections in *kernel b* to k^2 term only, but keep the complete contributions from the leading order.

In the NJL model, the constituent quarks are the fundamental elements, and the mesons are their bound. In fact, all the quantities in the NJL model are calculated from the quark propagator $S(p) = 1/(\not{p} - m)$. Therefor, if we want to build up a self-consistent expansion in the caculation of the the 2-loop diagrams, we should only expand the quark propagator in the external momentum k

$$S(p \mp k) = \frac{1}{\not{p} \mp \not{k} - m} = S(p) \pm S(p)\not{k}S(p) + S(p)\not{k}S(p)\not{k}S(p) + \cdots.\tag{15}$$

With this expansion, all the two-loop diagrams can be expanded naturally in k in a unified way.

The Lorentz covariance gives the expansion form of $\Pi_\pi(k)$ as

$$\begin{aligned}\Pi_\pi(k) &= \Pi_\pi^{(RPA)}(k) + \delta\Pi_\pi(k), \\ \delta\Pi_\pi(k) &= \delta\Pi_\pi(0) + k^2\delta\Pi_\pi^{(2)}(0) + k^4\delta\Pi_\pi^{(4)}(0) + \cdots.\end{aligned}\tag{16}$$

In the following, we consider $\delta\Pi_\pi(k)$ to the k^2 term only. In this approximation, the pole condition for the pion propagator is simplified as

$$1 - 2G(\Pi_\pi^{(RPA)}(k^2 = m_\pi^2) + \delta\Pi_\pi(0) + m_\pi^2\delta\Pi_\pi^{(2)}(0)) = 0.\tag{17}$$

With the expression of $\Pi_\pi^{(RPA)}(k)$ and the gap equation Eq. (2) we obtain the gap equation to determine the pion mass,

$$m_\pi^2 = \frac{m_0}{Gm(-8N_c i I(m_\pi) + 2\delta\Pi_\pi^{(2)}(0))}.\tag{18}$$

Similarly, the expansion of the residue of the pole to the order k^2 gives the pion-quark coupling constant

$$g_{\pi qq}^{-2} = (\partial\Pi_\pi^{(RPA)}(k)/\partial k^2)^{-1}|_{k^2=m_\pi^2} + \delta\Pi_\pi^{(2)}(0),\tag{19}$$

where $(\partial\Pi_\pi^{(RPA)}(k)/\partial k^2)^{-1} = -2N_c i(I(0) + I(k) - k^2 K(k))$, and the quark-loop integral $K(k)$ is defined in Appendix.

B. Calculation of $\delta\Pi_\pi^{(2)}(0)$

It is tedious to calculate $\delta\Pi_\pi^{(2)}(0)$ directly. Here we will use another equivalent way by calculating the first term of the axial-vector matrix element in the external momentum expansion.

We have shown the general relations between pion polarization function and axial-vector matrix element in Eq. (13). If $k^2 = 0$, i.e., in the chiral limit, Eq. (13) becomes

$$\frac{m_H}{2G} = m\Pi_\pi^{(RPA)}(0), \quad \frac{\delta m}{2G} = m\delta\Pi_\pi(0).\tag{20}$$

Thus the Eq. (13) in general case can be rewritten as

$$\frac{k^2 f_\pi^{(RPA)}(k)}{g_{\pi qq}(k)} = m(\Pi_\pi^{(RPA)}(k) - \Pi_\pi^{(RPA)}(0)), \quad \frac{k^2 \delta f_\pi(k)}{g_{\pi qq}(k)} = m(\delta\Pi_\pi(k) - \delta\Pi_\pi(0)),\tag{21}$$

With the expansion form of $\Pi_\pi(k)$, the second equation of (21) becomes

$$\frac{k^2 \delta f_\pi(k)}{g_{\pi qq}(k)} = m(k^2 \delta \Pi_\pi^{(2)}(0) + k^4 \delta \Pi_\pi^{(4)}(0) + \dots). \quad (22)$$

By replacing in the Feynman diagrams in *kernel b* one vertex $i\gamma_5 \vec{\tau}$ by $ig_{\pi qq}(k)\gamma_5\gamma_\mu \vec{\tau}/2$, the obtained subleading axial-vector matrix element has the following form in external momentum expansion:

$$\frac{k_\mu \delta f_\pi(k)}{g_{\pi qq}(k)} = k_\mu m(M(0) + k^2 M^{(2)}(0) + \dots). \quad (23)$$

Comparing the two equations (22) and (23), we derive the pion polarization fluctuation in terms of the first coefficient of the expansion of the axial-vector matrix element.

$$\delta \Pi_\pi^{(2)}(0) = M(0) = M^{(b)}(0) + M^{(c)}(0) + M^{(d)}(0) \quad (24)$$

with

$$\begin{aligned} M^{(b)}(0) = & i N_c \left\{ \int \frac{d^4 q}{(2\pi)^4} [-iD_\pi^{(RPA)}(q)](-3q^2 L(q)) \right. \\ & \left. + \int \frac{d^4 q}{(2\pi)^4} [-iD_\sigma^{(RPA)}(q)](4K(q) + 3(4m^2 - q^2)L(q)) \right\}, \end{aligned} \quad (25)$$

$$\begin{aligned} M^{(c)}(0) = & i N_c \left\{ 6 \int \frac{d^4 q}{(2\pi)^4} [-iD_\pi^{(RPA)}(q)](K(q) + 3K(0) - 3q^2 M(q)) \right. \\ & \left. + 2 \int \frac{d^4 q}{(2\pi)^4} [-iD_\sigma^{(RPA)}(q)](5K(q) + 3K(0) - 3(q^2 - 4m^2)M(q)) \right\}, \end{aligned} \quad (26)$$

$$\begin{aligned} M^{(d)}(0) = & -32iN_c \int \frac{d^4 q}{(2\pi)^4} N_c [-iD_\pi^{(RPA)}(q)] [-iD_\sigma^{(RPA)}(q)] \{ -(I(q) + 2m^2 K(0))(I(q) - I(0)) \\ & + (I(q) + I(0) - (q^2 + 2m^2)K(q))I(q) - q^2 I(q)(I(q) + 2m^2 K(0))[-iD_\sigma^{(1)}(q)] \}, \end{aligned} \quad (27)$$

where $L(q)$, $M(q)$ are defined in Appendix. In calculating $M^{(d)}(0)$, we have expanded the internal σ propagator as

$$[-iD_\sigma^{(RPA)}(q-k)] = [-iD_\sigma^{(RPA)}(q)](1 + q_\nu k^\nu [-iD_\sigma^{(1)}(q)] [-iD_\sigma^{(RPA)}(q)]), \quad (28)$$

with $[-iD_\sigma^{(1)}(q)] = 8N_c(I(q) + ((4m^2 - q^2)/2q^2)(I(q) - I(0) + q^2 K(q))[-iD_\sigma^{(RPA)}(q)])$.

C. Internal RPA Meson Propagator

Till now, we have assumed that *kernel a* and *kernel b* shown in Fig. 2 are expanded properly to leading and subleading order in N_c . In the chiral limit beyond mean-field approximation, the leading meson polarization function $\Pi_M^{(RPA)}$ has the order of $O(N_c)$, which gives the RPA meson propagator $D_M^{(RPA)}(q)$ in the order of $O(1/N_c)$, thus δm is the subleading $O(1/N_c)$ order of quark self-energy. However, it is not the case when current quark mass is introduced beyond mean-field approximation.

Now we first analyze the one-quark-loop pion propagator $D_\pi^{(RPA)}(q)$ beyond mean-field approximation and including m_0 explicitly. The definition of RPA pion propagator is

$$-iD_\pi^{(RPA)}(q) = \frac{2iG}{1 - 2G\Pi_\pi^{(RPA)}(q)}. \quad (29)$$

Substituting the expression of $\Pi_\pi^{(RPA)}(q)$, and using the gap equation Eq. (2), the denominator is

$$1 - 2G\Pi_\pi^{(RPA)}(q) = \frac{m_0 + \delta m}{m} + i8GN_c q^2 I(q). \quad (30)$$

With the pion pole condition Eq. (4), we can deduce

$$\frac{m_0 + \delta m}{m} = -i8GN_c m_\pi^2 I(m_\pi) + 2G\delta\Pi_\pi(m_\pi). \quad (31)$$

So the RPA pion propagator (29) can be expressed as

$$-iD_\pi^{(RPA)}(q) = \frac{1}{4N_c(-m_\pi^2 I(m_\pi) + q^2 I(q)) - i\delta\Pi_\pi(m_\pi)}. \quad (32)$$

Here $\delta\Pi_\pi(m_\pi)$ is the subleading diagrams' contribution, which is in the order of $O(1)$. This term induces the RPA propagator expanded to $O(1/N_c^n)$ order, where n could go to ∞ . If we substitute this complete form of internal pion propagator into *kernel a*, it is clear that the $O(1/N_c)$ part of RPA propagator corresponds to the $O(1/N_c)$ part of δm , and other suppressed parts of RPA propagator correspond to the suppressed parts of δm .

In order to keep the proper subleading order $O(1/N_c)$ of δm , the internal meson propagator must be in its leading order $O(1/N_c)$. We neglect the contributions resulted from $\delta\Pi_\pi(m_\pi)$, and get the leading order of pion propagator in $O(1/N_c)$,

$$-iD_{\pi}^{(RPA)}(q) = \frac{1}{4N_c(-m_{\pi}^2 I(m_{\pi}) + q^2 I(q))}. \quad (33)$$

Similarly, the $O(1/N_c)$ sigma propagator is

$$-iD_{\sigma}^{(RPA)}(q) = \frac{1}{4N_c(-m_{\pi}^2 I(m_{\pi}) + (q^2 - 4m^2)I(q))}. \quad (34)$$

It can be seen that G is not included explicitly in the two RPA meson propagators, and this simplifies our numerical calculations.

IV. NUMERICAL RESULTS AND DISCUSSION

Now we turn to the numerical evaluation. As evaluated in the last two chapters, we have three equations, the gap equation, Eq. (2), pion pole condition, Eq. (4), and pion decay constant, Eq. (14). In the chiral limit, pion pole condition Eq. (4) is trivial and the pion decay constant satisfies the Goldberger-Treiman relation.

In order to deal with the divergence resulted from quark-loop integral and meson-loop integral, like in [13], we introduce two cut-off, the quark momentum cut-off Λ_f in Pauli-Villars regularization and the meson momentum cut-off Λ_b in covariant regularization. As pointed out in Introduction, there are four parameters, the current quark mass m_0 , coupling constant G , quark momentum cut-off Λ_f and meson momentum cut-off Λ_b to be fixed. By comparing with two observables $m_{\pi} = 139\text{MeV}$, $f_{\pi} = 92.4\text{MeV}$ and one reasonable empirical range of $-300\text{MeV} < 1/2 < \bar{q}q >^{1/3} < -200\text{MeV}$, we can not give fixed values of these four parameters. Here we regard the ratio $z = \Lambda_b/\Lambda_f$ as one free parameter. For each z , we can get a series of solutions from the above conditions. The meson cloud effect is now characterized by z , the larger z means more meson contributions. Specially, when $z = 0$, i.e., $\Lambda_b = 0$, it returns to the mean-field approximation.

In the case of explicit chiral symmetry breaking $m_0 \neq 0$, giving a z , for different m , we find a series of Λ_f and m_0 from the above three equations, and then G , $< \bar{q}q >$ and other quantities could be calculated. In the case of chiral limit $m_0 = 0$, giving a z , for different m ,

we find Λ_f and G from Goldberger-Treiman equation and the gap equation, then $\langle \bar{q}q \rangle$ and other quantities are calculated.

In both cases, the mesonic contributions to the quark self-energy m and to the pion polarization $\Pi_\pi(k)$ are negative, and all the ratios of the mesonic corrections to the one-quark-loop contributions to m , $\Pi_\pi(k)$ and physical quantities f_π and quark condensate increases with increasing z , and can reach 30-40% for values of parameters in the range $0.3\text{GeV} < m < 0.5\text{GeV}$ and $1 < z < 1.5$. These results are qualitatively the same as those in [13] and [12].

Our numerical results are shown in Figs. 3-5, which concentrate on investigating the effect of explicit chiral symmetry breaking. In all figures, the solid lines correspond to the case of explicit chiral symmetry breaking $m_0 \neq 0$, and the dashed lines correspond to the case of chiral limit $m_0 = 0$, and a, b, c, d, e correspond to $z = 0, 0.5, 1, 1.5, 2$, respectively.

In Fig. 3, we plot the quark scalar condensate $(-1/2 < \bar{q}q >^{1/3})$ as a function of constituent quark mass m for different values of z . This figure is different from the Fig. 6 and Fig. 7 in [12]. Our numerical results show that:

- 1). For each curve, the quark condensate has a plateau, in which the quark condensate changes slowly with m , and the width of the plateau becomes more and more narrow with increasing z . For each curve, we define the plateau in the range of $(-1/2 < \bar{q}q >^{1/3}) < (-1/2 < \bar{q}q >_{min}^{1/3} + 0.0015)$ GeV.
- 2). For each z , the plateau of quark condensate is in the experimental range $0.2 \text{ GeV} \sim 0.3 \text{ GeV}$, and the plateau becomes higher and higher with increasing z , which shows that the meson contributions affect the quark condensate explicitly.
- 3). The solid and dashed lines of a are almost coincide, which means that the effect of current quark mass is invisible in the mean-field approximation. While beyond mean-field approximation, i.e., considering the meson contributions, the two curves in the case of b or c, d, e are separate in the region of the plateau.

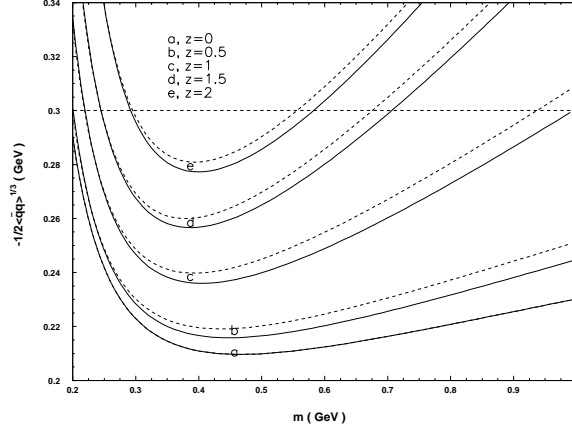


FIG. 3. Quark condensate $-1/2 < \bar{q}q >^{1/3}$ as a function of the constituent quark mass m for different values of $z = \Lambda_b/\Lambda_f$. The solid lines and dashed lines correspond to $m_0 \neq 0$ and $m_0 = 0$ respectively.

In Table 1, corresponding to the plateau region $(-1/2 < \bar{q}q >^{1/3}) < (-1/2 < \bar{q}q >_{min}^{1/3} + 0.0015)\text{GeV}$,

		$-\frac{1}{2} < \bar{q}q >^{1/3}$ (GeV)	m(GeV)	$m_0(\text{MeV})$	$\Lambda_f(\text{GeV})$	$G\Lambda_f^2$
z=0	$m_0 = 0$	0.2096+0.0015	0.47 \pm 0.1		0.615 \pm 0.002	4.8 \pm 0.9
	$m_0 \neq 0$			8.9 \pm 0.30		
z=1	$m_0 = 0$	0.2397+0.0015	0.39 \pm 0.05		0.725 \pm 0.01	4.8 \pm 0.5
	$m_0 \neq 0$	0.2360+0.0015	0.40 \pm 0.05	7.78 \pm 0.20	0.71 \pm 0.01	4.7 \pm 0.5
z=1.5	$m_0 = 0$	0.2599+0.0015	0.38 \pm 0.04		0.801 \pm 0.008	5.3 \pm 0.5
	$m_0 \neq 0$	0.2566+0.0015	0.39 \pm 0.04	7.29 \pm 0.20	0.785 \pm 0.008	5.2 \pm 0.5

Table. 1. Quantities in the region of defined plateaus.

we list the range of constituent quark mass m , current quark mass m_0 , quark momentum cut-off Λ_f and a dimensionless quantity $G\Lambda_f^2$. This table shows that, in the mean-field approximation, the values of constituent quark mass m and the current mass m_0 in the plateau is a little higher than the empirical values $m \simeq 1/3$ *proton mass* and $m_0 \simeq 5 \sim 7$ MeV, and the quark condensate in the plateau is much lower than 0.25 GeV; however, these quantities in the plateaus at $z = 1, 1.5$ are more reasonable comparing with the empirical values.

In Fig. 4, we show the quark momentum cut-off Λ_f as a function of the constituent quark mass m ,

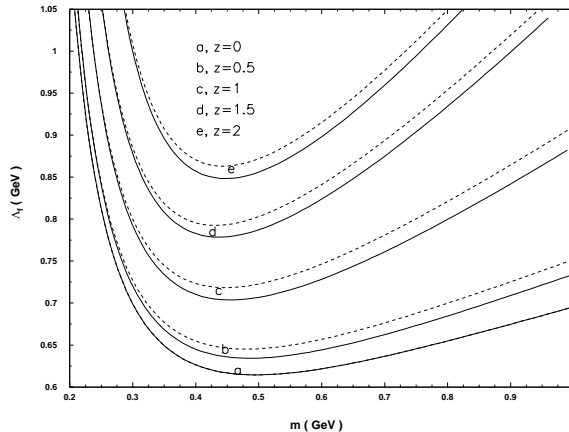


FIG. 4. Quark momentum cut-off Λ_f as a function of the constituent quark mass m for different values of $z = \Lambda_b/\Lambda_f$. The solid lines and dashed lines correspond to $m_0 \neq 0$ and $m_0 = 0$ respectively.

and in Fig. 5 we show the current quark mass m_0 as a function of the constituent quark mass m for different values of z . There is also a plateau for each curve. Although the ranges of constituent quark mass m corresponding to the Λ_f plateau, m_0 plateau and quark condensate plateau are not exactly the same, they are mostly around $m = 0.4 \pm 0.1$ GeV. This range $m = 0.4 \pm 0.1$ GeV is determined dominantly by the gap equation in the mean-field approximation, the effects of meson cloud contributions are also shown clearly. Comparing

the plateaus at $z = 0$ and $z = 1.5$, we see that Λ_f and $(-1/2 < \bar{q}q >^{1/3})$ are all modified by the order of about 30%. But the corresponding plateaus at $z = 2$ modified too much. In fact, all these figures show that the plateaus of $z = 2$ are abnormal comparing that of $z = 0.5, 1, 1.5$. Based on the above analysis, it seems that $z = 2$ is not a reasonable choice, and $z = 1 \sim 1.5$ is more reasonable.

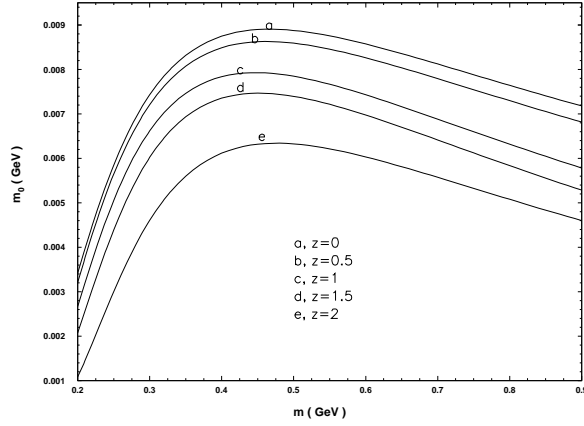


FIG. 5. Current quark mass m_0 as a function of the constituent quark mass m for different values of $z = \Lambda_b/\Lambda_f$. The solid lines and dashed lines correspond to $m_0 \neq 0$ and $m_0 = 0$ respectively.

In the region $m = 0.4 \pm 0.1$ GeV, all these three figures Figs. 3-5 show that:

- 1) In the mean-field approximation, the solid line and dashed line of $z = 0$ coincide, which means that the effects of the current quark mass are invisible in this case.
- 2) When beyond mean-field approximation $z > 0$, i.e, considering meson contributions, the effects of current quark mass are explicitly reflected by the separation of the solid and dashed lines.

As we pointed out in Introduction, in NJL model all information is calculated from constituent quark propagator, and the current quark mass m_0 induces the massive pion m_π . In the mean-field approximation, there is no feedback of meson modes to quark propagator, so the effects of m_0 or m_π can not be reflected. Only beyond mean-field approximation, when

the back interaction of meson mode to quark propagator are considered, can the effects of m_0 or m_π be reflected on the quantities calculated from the fundamental element, quark propagator.

V. CONCLUSIONS AND SUMMARY

We establish a general scheme of SU(2) NJL model including the current quark mass explicitly and considering the meson cloud contributions. To ensure the quark self-energy expanded in the proper order of $1/N_c$, we discuss in details that the internal meson propagator must be in $O(1/N_c)$ order. And we also develop a unified way to calculate all Feynman diagrams in the NJL model by only expanding the constituent quark propagator in external momentum k . Our numerical results show that: a) when $z = 1 \sim 1.5$, the NJL parameters are more reasonable than that in the mean-field approximation; b) the effect of current quark mass can be reflected only beyond mean-field approximation, and it is characterized explicitly by the separation of the solid and dashed lines in the range of the parameters corresponding to m between $0.3\text{GeV} \sim 0.5\text{GeV}$.

ACKNOWLEDGMENTS

The authors would like to thank Dr. V. Dmitrašinović, Dr. E.N. Nikolov and Dr. M. Franz for their kind help during this work. This work is supported by NNSF of China (Nos. 19677102 and 19845001).

APPENDIX: Definition of Integral Functions and Corresponding Pauli-Villars Expressions

The fundamental functions are defined as following:

$$F = \int \frac{d^4 p}{(2\pi)^4} \frac{1}{p^2 - m^2}, \quad (1)$$

$$I(q) = \int \frac{d^4 p}{(2\pi)^4} \frac{1}{(p^2 - m^2)((p + q)^2 - m^2)}, \quad (2)$$

$$K(q) = \int \frac{d^4 p}{(2\pi)^4} \frac{1}{(p^2 - m^2)^2((p + q)^2 - m^2)}, \quad (3)$$

$$L(q) = \int \frac{d^4 p}{(2\pi)^4} \frac{1}{(p^2 - m^2)^2((p + q)^2 - m^2)^2}, \quad (4)$$

$$M(q) = \int \frac{d^4 p}{(2\pi)^4} \frac{1}{(p^2 - m^2)^3((p + q)^2 - m^2)}, \quad (5)$$

And their corresponding Pauli-Villars expressions are:

$$F_{PV} = -\frac{i}{(4\pi)^2} \sum_a C_a M_a^2 \ln \frac{M_a^2}{m^2}, \quad (6)$$

$$I(q)_{PV} = \frac{i}{(4\pi)^2} \sum_a C_a \left(-\ln \frac{M_a^2}{m^2} + 2(1 - \sqrt{1 + y_a^{-1}}) \ln(\sqrt{y_a} + \sqrt{1 + y_a}) \right), \quad (7)$$

$$K(q)_{PV} = -\frac{i}{(4\pi)^2} \sum_a C_a \frac{1}{2M_a^2} \frac{\ln(\sqrt{y_a} + \sqrt{1 + y_a})}{\sqrt{y_a}(1 + y_a)}, \quad (8)$$

$$L(q)_{PV} = \frac{i}{(4\pi)^2} \sum_a C_a \left(-\frac{1}{8M_a^4 y_a (1 + y_a)} \right) \left(1 - \frac{1 + 2y_a}{\sqrt{y_a}(1 + y_a)} \ln(\sqrt{y_a} + \sqrt{1 + y_a}) \right), \quad (9)$$

$$M(q)_{PV} = \frac{i}{(4\pi)^2} \sum_a C_a \left(\frac{1}{16M_a^4 y_a (1 + y_a)} \right) \left(1 + 2y_a - \frac{\ln(\sqrt{y_a} + \sqrt{1 + y_a})}{\sqrt{y_a}(1 + y_a)} \right), \quad (10)$$

where $C_a = [1, 1, -2]$, $\alpha_a = [0, 2, 1]$, $M_a^2 = m^2(1 + \alpha_a x)$ for $a=0,1,2$, and $y_a = -q^2/(4M_a^2)$.

REFERENCES

- [1] Y. Nambu and G. Jona-Lasinio, Phys. Rev. **122**, 345 (1961); **124**, 246 (1961).
- [2] U. Vogl and W. Weise, Prog. Part. Nucl. Phys. **27**, 195 (1991);
- [3] S.P. Klevansky, Rev. Mod. Phys. **64**, 649 (1992);
- [4] T. Hatsuda and T. Kunihiro, Phys. Rep. **247**, 221 (1994).
- [5] T.H. Hansson, M. Prakash and I. Zahed, Nucl. Phys. **B 335**, 67(1990).
- [6] V. Bernard and U.-G. Meißner, Phys. Lett. **B 266**, 403(1991).
- [7] C. Schüren, E.Ruiz Arriola and K. Goeke, Nucl. Phys. **A 547**, 612(1992).
- [8] Nan-Wei Cao, C.M.Shakin, Wei-Dong Sun, Phys. Rev. **C 46**(1992) 2535.
- [9] E.Quack, S.P.Klevansky, Phys. Rev **C 49**(1994) 3283.
- [10] P.Zhuang, J.Hüfner, S.P.Klevansky, Nucl. Phys. **A 576**(1994)525.
- [11] D.Ebert, M.Nagy, M.K.Volkov, hep-th/9412214, JINR preprint E2-94-488.
- [12] E.N. Nikolov, W. Broniowski, C.V. Christov, G. Rippl and K. Goeke, Nucl. Phys. **A 608**, 411 (1996).
- [13] V. Dmitrašinović, H.-J. Schulze, R. Tegen and R.H. Lemmer, Ann.Phys. **238**, 332 (1995).
- [14] K.Akama, Nucl. Phys. **A 629** 37c(1998)
- [15] V. Bernard and D. Vautherin, Phys. Rev. **D 40**(1989),1615.
- [16] A. Dobado and J.R. Peláez, hep-ph/9807337.
- [17] E. Witten, Nucl. Phys. **B 160**, 57 (1979).